Available online at www.sciencedirect.com

ScienceDirect

Solar Energy 107 (2014) 245–259

SOLAR ENERGY

www.elsevier.com/locate/solener

A multi-agent-based energy-coordination control system for grid-connected large-scale wind–photovoltaic energy storage power-generation units

Kehe Wu [a], Huan Zhou [b,*]

[a] State Key Laboratory of Alternate Electrical Power System with Renewable Energy Sources, North China Electric Power University, No. 2 Beinong Road, Changping District, Beijing 102206, China

[b] School of Control and Computer Engineering, North China Electric Power University, No. 2 Beinong Road, Changping District, Beijing 102206, China

Received 8 February 2014; received in revised form 8 May 2014; accepted 9 May 2014
Available online 28 June 2014

Communicated by: Associate Editor Yogi Goswami.

Abstract

A multi-agent-based energy-coordination control system (MA-ECCS) is designed for grid-connected large-scale wind–photovoltaic energy storage power-generation units (WPS-PGUs) to address the challenges of low operation efficiency, poor stability, and complex decision making. The proposed system adopts the negotiation model of the contract net protocol with the non-fixed client–server cooperative mechanism among agents. When the power supply and demand are imbalanced, the system selects the state-changeable agent as the task initiator according to the load balance principle. In the energy-coordination process, the proposed system solves the global optimal-energy distribution plan of the system by considering the self-constraint and control objective of each agent and by using the improved particle swarm algorithm to achieve the maximum economic benefit on the basis of stable operations. The paper presents the overall design idea of the system, the agent models of different equipment, and the global energy-coordination optimization algorithm. An example is given to discuss the behavior characteristics of the agent and communication negotiation process and to verify that the system designed in this paper can realize the energy-coordination dispatching flexibly and efficiently. The method adopted by the system can improve the overall operation efficiency and economic benefits of WPS-PGUs.

Keywords: Wind–PV energy storage; Energy-coordination; Contract net protocol; Particle swarm algorithm

1. Introduction

The development of clean energies such as wind power and photovoltaic power has motivated many experts to study wind, photovoltaic, energy storage, power generation, and energy-coordination control systems. However, the operation process of large-scale wind, photovoltaic, energy storage, and power-generation units often suffer from low operation efficiency, poor stability, and lack of energy-coordination control strategies. Various countries around the world have successively conducted a number of demonstration projects showing improved intermittent power controllability by using energy storage technology (Campoccia et al., 2009; Mohammadi et al., 2012; Askarzadeh, 2013; Merei et al., 2013; Bayod-Rújula et al., 2013). Such tests are done in the peak and valley adjustments (Li et al., 2012) and in the adjustment and

* Corresponding author. Tel.: +86 010 61772791; fax: +86 010 61772747.
E-mail addresses: epuwkh@126.com (K. Wu), shenarder@163.com (H. Zhou).

http://dx.doi.org/10.1016/j.solener.2014.05.012
0038-092X/

improvement of power quality (Golovanov et al., 2013). In terms of energy-coordination control, the United States, Spain, and Denmark can optimize wind power and photovoltaic power under existing economic leverage on the basis of perfect electric power market mechanisms. By contrast, developing countries with backward market mechanisms are inexperienced in energy-coordination control. Therefore, the design of the energy-coordination control system can be applied to large-scale renewable-energy power-generation units to optimize output according to the distribution characteristics of natural resources. Furthermore, the output characteristics of the power-generation equipment are conducive for improving the power supply reliability and economic benefits of the power-generation unit and for promoting the development of energy sustainability.

Traditional grid-connected energy-coordination control of wind–photovoltaic energy storage generation plant uses a centralized energy management strategy based on intelligent control algorithm. With the increasing construction of wind farms and photovoltaic arrays, as well as the increasing adoption of composite energy storage systems, the defects of the centralized energy control method in flexibility and extensibility hinders the operations of large-scale integrated power-generation systems for wind, photovoltaic, and energy storage units. The multi-agent system, which responds intelligently and flexibly to changes in working conditions and requirements, has been widely applied in various aspects of the power system (Kremers et al., 2013; da Rosa et al., 2012; Pipattanasomporn et al., 2012).

To date, the MAS-based energy-coordination control strategy mainly includes the optimal scheduling strategy based on the intelligent algorithm and the competition coordination strategy based on free market trading. The former provides the overall optimization objectives of the system and the constraints of the equipment, provides the equipment operation parameters and real-time load demand, and determines the energy-coordination scheme with the intelligent algorithm. For example, by reducing the operating costs and NO_x emissions as the objectives, Roche et al. (2012) considers economic and environmental constraints in the design of a MAS-based energy management system for a gas turbine power plant and validates the flexibility and efficiency of the system by providing an example. Jun et al. (2011) uses the minimum cost and operation reliability of the system as objectives to propose a solution for MAS-based distributed renewable-energy hybrid power-generation systems. The solution designs the behavior of the agent with the operation characteristics of the equipment and realizes a large MAS system based on the JADE environment, thus proving the rationality of the MAS in the energy-coordination control of the renewable-energy hybrid power-generation system. By using high fault tolerance, openness, and adaptability as the objectives, Lagorse et al. (2010) adopts the bottom-up approach to design a MAS-based distributed power-generation management system and verifies by simulations that this system is more efficient in handling problems than centralized energy management systems. Jiang (2008) uses high energy density, power density, and combustion efficiency as the objectives to design a MAS-based hybrid-power energy-coordination plan and proves the high efficiency and robustness of the system by simulations. Logenthiran et al. (2011) uses the minimized operation cost as the objective to design the energy-coordination strategy of distributed power-generation under an isolated environment based on MAS. The system uses three-stage energy dispatching strategies to maximize the use of renewable energies, to meet the demands of each independent micronetwork system and the overall requirements, and to minimize operation costs.

The free market trading-based competition coordination method simulates the tendering/bidding/bid winning mechanism. Each output equipment bids for the tendering control unit, and the tendering control unit achieves energy coordination based on the competitiveness of the bidding unit. For instance, Logenthiran et al. (2008) sets the market operator as the internal consultation control center under a microenvironment in the energy market. Dimeas and Hatziargyriou (2005) establishes three layers of control system under the micronetwork environment and designs MO, MGCC, and other agents to manage the internal consultation process in the energy market.

On the basis of existing research results, this paper presents the design of a multi-agent-based energy-coordination control system that enhances flexibility and extensibility of power-generation units with non-fixed client–server cooperative mechanism. The proposed system simulates the bidding mechanism in the market by using the contract network protocol. By considering the self-constraint and interests, the proposed system solves the global optimal-energy distribution plan of the system by the improved particle swarm algorithm to achieve the maximum economic benefit on the basis of stable operations. The paper focuses on the development of grid-connected MA-ECCS for optimizing the performance of large-scale wind–photovoltaic energy storage power-generation units based on the following steps:

(1) Design the architecture of multi-agent system based on the physical structure of wind–photovoltaic energy storage power-generation units, determine the overall system coordination mechanism and communication protocol.
(2) Develop corresponding control strategies according to the output characteristics of different power-generation equipment.
(3) Determine the system global optimization objective and energy coordinated control strategy.
(4) Achieve the overall optimal objective under the premise of meeting the demand of meteorological conditions, load, constraints of various aspects and personal interests, develop energy coordinated control process.

(5) Verify the economic benefit and operating stability of multi-agent system based on the case study.

2. System structure

2.1. Structure of the large-scale WPS-PGUs

The structure of the typical large-scale *WPS-PGUs* is shown in Fig. 1. The wind turbine, photovoltaic array and batteries are connected to the DC bus through the converter and the bus is connected to the power grid through the inverter and the step-up transformer in the substation. The wind turbine and photovoltaic array mainly convert renewable energy sources such as wind energy and solar energy into electric energy; the batteries are used for energy regulation, and load balance. The energy coordination control system arranges the output of the power generation device according to the requirements of the grid and the meteorological conditions, thus realizing the stable grid-connected operation of the power generation unit.

2.2. The structure of the MA-ECCS

Four Agents are designed in the paper, including Wind Turbine (WT) Agent, Photovoltaic (PV) Agent, Battery (BAT) Agent and Load (LD) Agent. Each Agent can control several generating unit of the same characteristics and determine its own control objective according to the characteristics of the equipment. The structure of MA-ECCS is shown in Fig. 2.

The system adopts the non-fixed client–server cooperative mechanism. Facing the conditions such as changes of the demand of the power grid and the meteorological, the joining or quitting of the units, and the imbalanced supply and demand between the power generation unit and the power grid, the corresponding Agent should initiate the energy coordination task as the control center to ensure the stable grid-connected operation of the system. The Agent initiating the energy coordination task is considered to be the Task Agent. Other Agents determine how to participate in the energy coordination according to their own characters and control objectives. In order to avoid the conflict caused by several Agents initiating the energy coordination tasks at the same moment, the timestamp Task-Token is set to be the symbol of Task Agent. Only the Task Agent with Task-Token in the effective period of time can initiate the energy coordination task.

The FIPA97-based contract net protocol (Smith, 1980) is adopted between Agents to be the way of communication and the quad data $<E, B, C, S>$ is designed to be the bidding data submitted by the participants to the initiators. Among them, E represents the economic parameters of the equipment, such as the operation cost, and depreciation cost; B represents the bid value of the active output which can be a constant or a scope; C is the constraint condition, such as the maximum output power of the equipment, the capacity and service life of the batteries. S is the running state of the equipment, such as running, hot standby, cold standby, and downtime.

3. Agent modeling and characteristic analysis

3.1. Basic structure of Agent

Fig. 3 shows the internal structure of the typical Agent. Agent feels the change of environment through the perception module and responds to the environment through the action module. Inference and decision making are the core modules of Agent on the basis of the local model/algorithm library and knowledge library. During the Inference process, the constraint condition, task standard, current token location and abilities of other Agents will be combined to make decisions or make decisions after negotiation with other Agents. In the decision-making process, it realizes the experience accumulation and organization and achieves the purpose of autonomous learning.

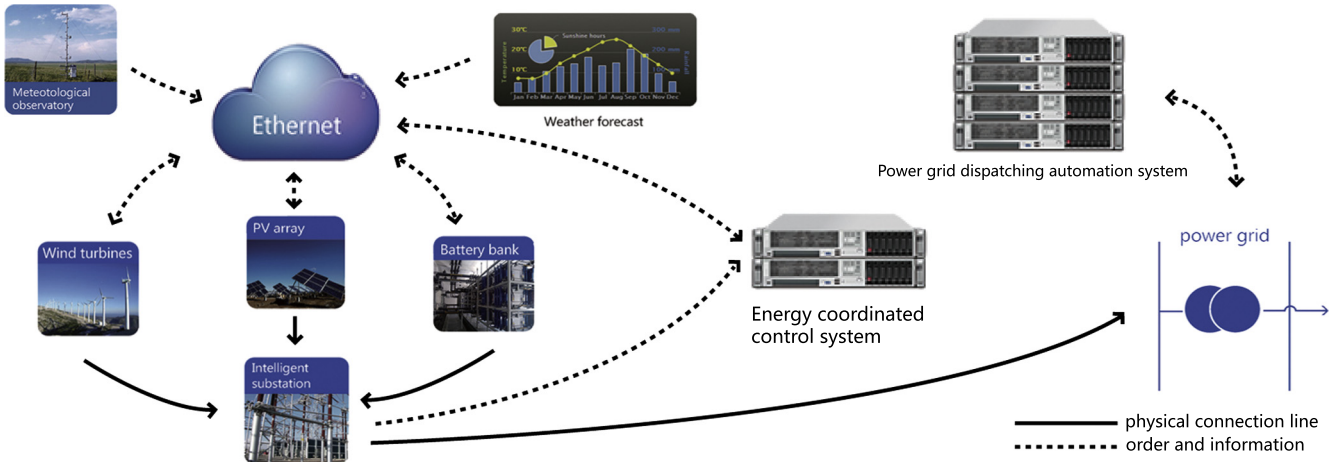

Fig. 1. The structure of the typical large-scale WPS-PGUs.

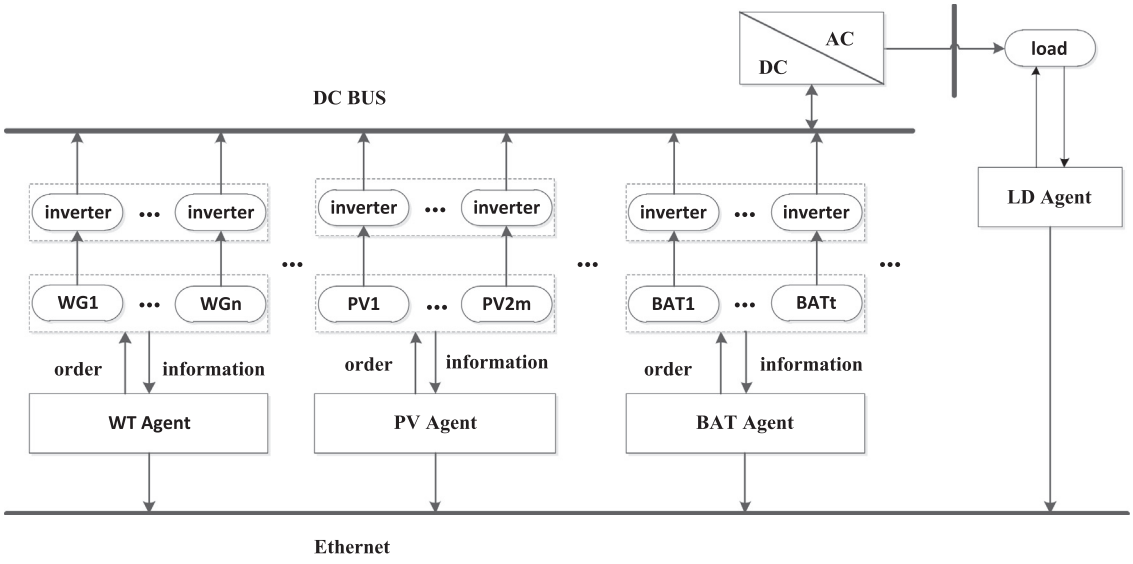

Fig. 2. The structure of MA-ECCS.

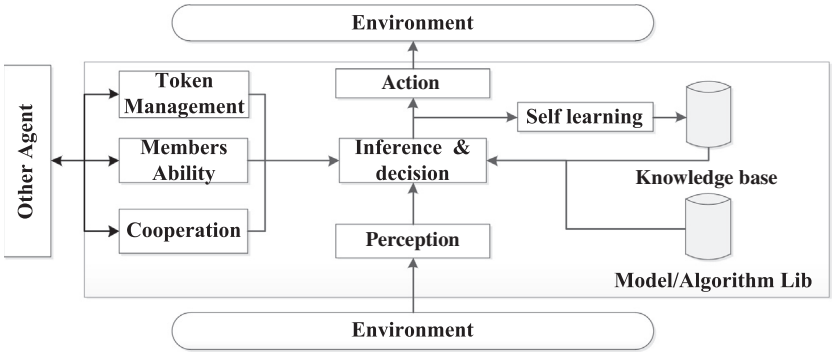

Fig. 3. Basic structure of Agent.

3.2. Characteristics of Agent

3.2.1. WT Agent and PV Agent

WT Agent and PV Agent represent the control units of the wind turbine and the photovoltaic panel, respectively. As the wind turbine and the photovoltaic panel operate at a low levelized cost, in the principle of maximizing the use of renewable energy, the characteristics of WT Agent and PV Agent are designed to be participating in the bidding actively until all the available equipment operate to the maximum power output. At the same time, they can initiate the energy coordination task when the power output changes.

The output power characteristics of the wind generator can be expressed as (Yang et al., 2009):

$$P_{WT}(k)=\begin{cases}0 & v(k)<v_{\min}\ \text{or}\ v(k)>v_{\max}\\ P_{rated} & v_{rated}\leqslant v(k)\leqslant v_{\max}\\ P_{rated}\frac{v(k)^2-v_{\min}^2}{v_{rated}^2-v_{\min}^2} & v_{\min}\leqslant v(k)<v_{rated}\end{cases} \tag{1}$$

where $P_{WT}(k)$ is the output power of the wind generator at time k; P_{rated} is the rated power of the wind generator; $v_{\min}$, $v_{\max}$, and v_{rated} are the minimum start-up wind speed, cutoff wind speed, and minimum rated wind speed of the wind generator.

The output power model of the PV module is determined by solar radiation and environmental temperature (Kazem and Khatib, 2013), as follows:

$$P_{PV}(t)=A_{pv}G(t)\eta_{pv}(t)\eta_{inv} \tag{2}$$

where A_{pv} (m^2) is the area of the PV panel exposed to solar radiation, $G(t)$ (W/m^2) is the value of solar radiation, $\eta_{pv}(t)$ is the energy conversion efficiency of the PV module, and η_{inv} is the conversion efficiency of the inverter. $\eta_{pv}(t)$ is influenced by environmental temperature:

$$\eta_{pv}(t)=\eta_{ref}[1-\beta(T_C(t)-T_{C_{ref}})] \tag{3}$$

$$T_C(t)-T_{ambient}=\frac{T_{rated}}{800}G(t) \tag{4}$$

η_{ref} is the reference energy conversion efficiency of the PV module under a standard temperature, β is the influence

coefficient of the temperature for energy conversion efficiency, $T_C(t)$ is the temperature of the PV module at t, and $T_{C_{ref}}$ is the reference standard temperature of the PV module, $T_{ambient}$ is the ambient temperature, and T_{rated} is the rated temperature of the PV module.

The output constraints of equipment can be expressed as:

$$0 \leqslant P_{WT}(t) \leqslant P_{WT}^{\max} \tag{5}$$

$$0 \leqslant P_{pv}(t) \leqslant P_{pv}^{\max} \tag{6}$$

where $P_{WT}^{\max}$ and $P_{pv}^{\max}$ are the upper power output limit of wind turbine and the photovoltaic panel.

After receiving the invitation to tender, WT Agent and PV Agent first search the relevant meteorological information of the current monitoring points and their own power output and calculate the maximum power output at this moment according to Eqs. (1)–(6) which is sent back as the B value of the bid document. When the unit fails to work or stops for general maintenance, WT Agent and PV Agent can turn off the equipment based on ensuring their own safe operation.

3.2.2. Battery Agent

BAT Agent in the system can monitor the state of charge (SOC) of the battery and manage the charge and discharge of the batteries. It can be divided into the following two types according to its response characteristics: the control objective of the first one, ECO-BAT Agent, is to maximize economic benefits. When responding to the energy coordination task initiated by Task Agent, ECO-BAT Agent will take full consideration to the price information of the current load demand and determine the bid value B according to its own SOC state. It does not receive the change of Task Agent; the control objective of the second one, EME-BAT Agent, is to maximize the power supply reliability. When responding to the energy coordination task, it will consider the current SOC state and then determine the maximum charge and discharge interval as the bid value B. At the same time, it receives any valid value in the interval coordinated by Task Agent.

The output power model of the battery is (Yang et al., 2007):

(1) Charge:

$$SOC(t+1) = SOC(t) \cdot (1-\sigma) + \frac{P_{CH}(t) \cdot \Delta t \cdot \eta_{CH}}{E_{bat}} \tag{7}$$

(2) Discharge:

$$SOC(t+1) = SOC(t) \cdot (1-\sigma) - \frac{P_{DIS}(t) \cdot \Delta t}{E_{bat}\eta_{DIS}} \Delta t \tag{8}$$

$SOC(t)$ is the battery state of charge after t; σ is the self-discharge per hour of the battery; P_{CH} and P_{DIS} are the charge and discharge powers of the battery in t, respectively; Δt is the length of t; η_{CH} and η_{DIS} are the charge and discharge efficiencies of the battery, respectively; and $E_{\max}$ is the maximum capacity of the battery.

The battery state of charge must be kept in a reasonable range:

$$SOC_{\min} \leqslant SOC(t) \leqslant SOC_{\max} \tag{9}$$

where $SOC_{\min}$ and $SOC_{\max}$ are minimum and maximum of battery capacity.

The modeling of the life cycle of a battery will affect the calculation of total system cost. The present study adopts the method of Lopez (Dufo-Lopez and Bernal-Agustin, 2008), which estimates cycles to failure of batteries by calculating the number of charge and discharge within an interval of several discharge depths (Fig. 4). The calculation method is as formula 10:

$$Life_{bat} = \frac{n_T \Delta t}{8760 \times \sum_{t=1}^{n_T} \sum_{m=1}^{M} (N_m(t)/CF_m)} \tag{10}$$

where $Life_{bat}$ is the failure cycle of the battery (year); Δt is the length of the statistical cycle length (h); n_T is the total number of time intervals of the simulation; $N_m(t)$ is the times of charge and discharge of the battery at the mth depth interval in the tth statistical cycle; CF_m is the total cycles of charge and discharge at the mth depth interval. Thus, the usage cycle of the battery CF_{bat} is not greater than its life cycle CTF_{bat}:

$$CF_{bat} \leqslant CTF_{bat} = min\{Life_{bat}, Life_{float}\} \tag{11}$$

$Life_{float}$ in the equation is the float cycle of the battery which is provided by the manufacturer.

In order to realize the behavior characteristics of BAT Agent, the fuzzy control method (Ding et al., 2013; Lagorse et al., 2009) is used to be the decision making mechanism of ECO-BAT Agent in the paper. With strong autonomy, ECO-BAT Agent can decide its own charge and discharge state and rate according to the time interval. When the load demand is high, leading to the higher price of the electricity, ECO-BAT Agent will make the discharging decision; instead, if both the load demand and the price of electricity are low, ECO-BAT Agent will make the charging decision. Therefore, the current electricity price (EP) and the capacity of the battery (SOC) are designed to be the decision inputs of ECO-BAT Agent and standardized to the interval [0, 1] and the output power of the battery is designed to be the decision output and standardized to the interval [−1, 1]; [−1, 0) and (0, 1] represent charge and discharge interval, respectively, 0 referring to be no action. The input and output membership functions are constructed as shown in Fig. 5, the control rules are shown in Table 1. The corresponding parameter fuzzy language variables are: very low (VL), low (L), medium (M), high (H), very high (VH), negative high (NH), negative medium (NM), negative low (NL), zero (ZE), positive low (PL), positive medium (PM), positive high (PH).

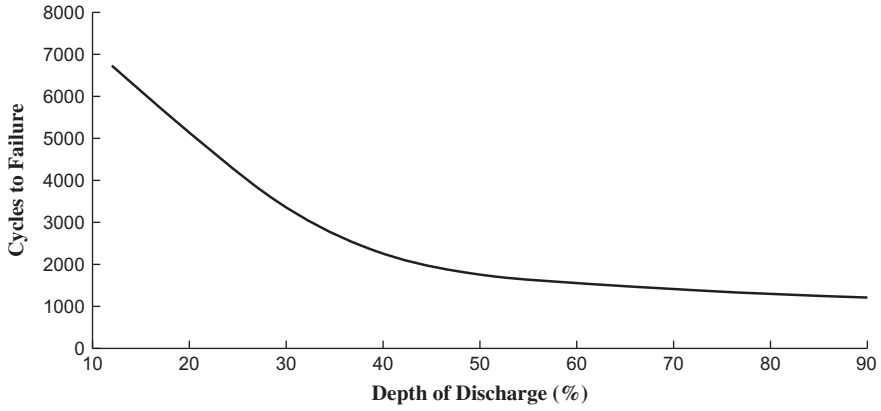

Fig. 4. The model of the life cycle of a battery.

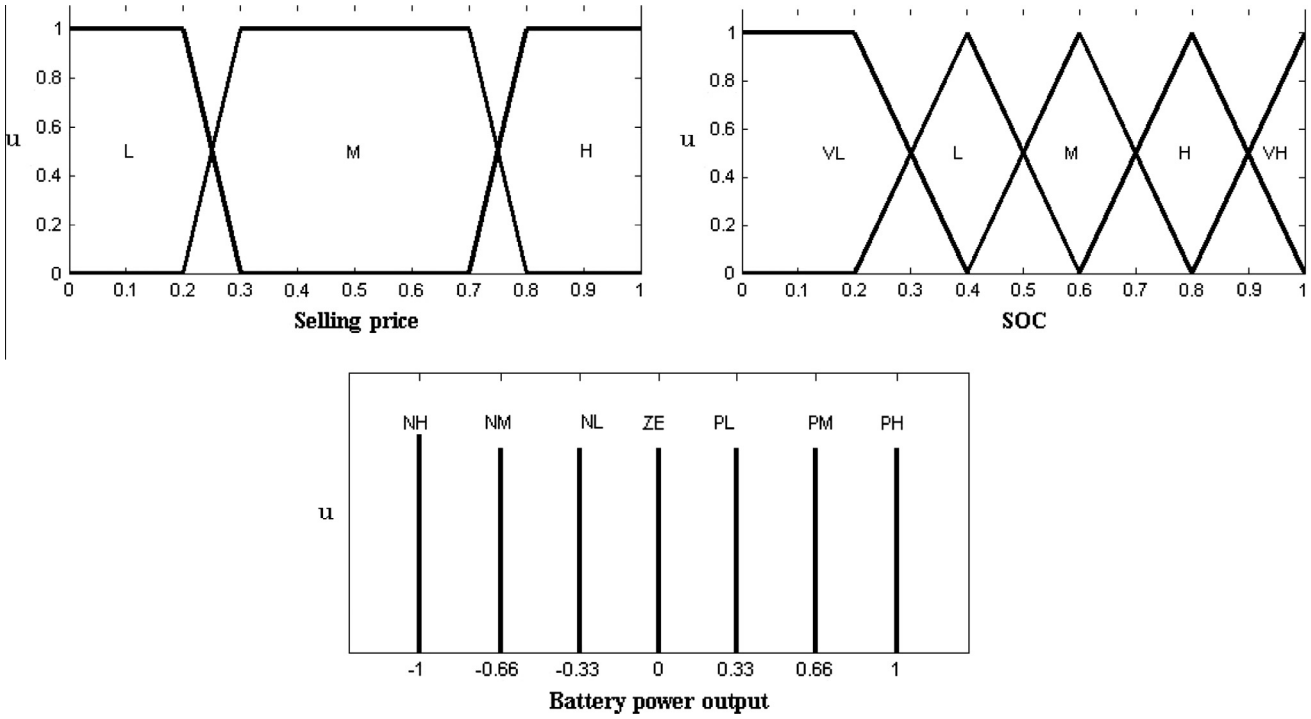

Fig. 5. Membership function of ECO-BAT.

The decision making method of EME-BAT Agent is relatively simple. After receiving the bidding requirements of Task Agent, it determines the charge and discharge interval $[-P_{CH\_MAX}(t),\ P_{DIS\_MAX}(t)]$ to be the bid value B according to Eqs. (7) and (8) and accepts any valid value in the interval distributed by Task Agent.

Table 1
Rule of fuzzy control.

EP/SOC	VL	L	M	H	VH
L	NH	NM	NM	NL	ZE
M	NM	NL	ZE	PL	PM
H	ZE	PL	PM	PM	PH

3.2.3. LD Agent

With satisfying the load demand of the power grid as the control objective, LD Agent can make the real-time monitoring of the change of the load and classify the load priorities according to the importance and can cut the less important load when the power generation unit cannot meet the load demand of the power grid.

When the load demand of the power grid changes, LD Agent can also apply for Task Agent to initiate the energy coordination task. It deserves noting that when LD Agent receives the bid invitation and becomes the participant, it will regard the current load demand and the electricity price as the bid value B to send back. After the global energy coordination by Task Agent, if the returned bid

value R is 0, it suggests the balanced energy coordination; if the returned bid value R is greater than zero, it shows that the power generation unit cannot meet the load demand of the power grid. At this time, LD Agent will cut the less important load at Power R.

4. Objective and strategies of global coordination control

4.1. Objective function

The objective of the WPS-PGUs is to maximize the overall economic benefit of the system F in the study period T:

$$\max F = P_{sub}\int_0^T Pdt - [C_{OP}(P) + C_{DEP}(P) + C_{PUN}] \tag{12}$$

where P refers to the total output of the power generation unit; P_{sub} is the Feed-In Tariff; $C_{OP}(P)$, $C_{DEP}(P)$ and C_{PUN} refer to the overall operation cost and depreciation cost of the equipment and the penalty cost for load cutting in the research period, respectively. The calculation method is as follows:

$$C_{OP}(P) = C_s(P) + C_{om}(P) + C_m(P) \tag{13}$$

$$C_{DEP}(P) = \sum_{i=1}^{N}\left[\frac{C_{INS}^i}{L\times 24\times 365}\right] \tag{14}$$

$$C_{PUN} = \sum_{k=1}^{m}\int_0^{T_0}\alpha_k P_{cut}(t)dt \tag{15}$$

where C_s, C_{om} and C_m refer to the switching cost, operation maintenance cost and outage maintenance cost of the equipment, respectively; C_{INS}^i refers to the installation cost of Equipment i; L refers to the years of life loss of Equipment i; k refers to the no. of the time period when cutting the load; α_k and $P_{cut}(t)$ refer to the penalty factor of the load cutting and the power value of the cut load at the time period k.

The only constraint of the system is that the power generation unit should meet the scheduling demand of the power grid at any time of the research period:

$$\begin{cases} P_{wd}(t) + P_{pv}(t) + P_{bat}(t) = P_{ref}(t) \\ \forall t, t \in (0, T] \end{cases} \tag{16}$$

where $P_{ref}(t)$ refers to the expected output at time t.

4.2. The global energy coordination control algorithm

The particle swarm algorithm is used in the paper to solve the global optimal energy allocation plan. It is developed from the global optimization algorithm which was proposed by Dr. Eberhart and Dr. Kennedy in 1995 with the characteristics of strong optimization ability and fast convergence rate (Eberhart and Kennedy, 1995). However, traditional particle swarm optimization may fall into local optimal solution due to premature convergence during the iteration process. The paper improves the search efficiency and the global search ability of the algorithm through improving the aspects such as inertia weight, learning factor and mutation particle. The steps of the algorithm are as follows:

Step 1: define each particle to be the k–D space vector, indicating that the number of Agents involved in the energy coordination is assumed to be k, expressed as:

$$X = [x_1, x_2, \cdots x_k]^T \tag{17}$$

where x_k refers to the component of the particle in the kth dimension, representing the output value of Agent.

Step 2: take C in the quad data submitted by each Agent as the output constraint of each dimension; Eq. (16) is the constraint of the global output, which randomly and evenly generates m groups of particles (Eq. (18)):

$$P = \begin{cases} X_1 = [x_{11}, x_{12}, \cdots, x_{1k}]^T \\ \vdots \quad \vdots \quad \vdots \quad \vdots \\ X_m = [x_{m1}, x_{m2}, \cdots, x_{mk}]^T \end{cases} \tag{18}$$

where x_{mk} refers to the component of the kth dimension location of the mth particle X_m. The initial population P is obtained. If the particles cannot be generated to meet Eq. (16), the maximum output bid notice will be returned to each Agent. The difference between the load demand and the sum of the maximum outputs of each Agent is calculated to be the load cutting amount which is sent to GD Agent.

Step 3: calculate the particle fitness with E in the quad data submitted by each Agent as the basis and Eq. (19) as the objective:

$$Fit(x) = F \tag{19}$$

where F is calculated by Eq. (12).

Step 4: sort the particle fitness from big and find the optimal particle and the optimal location:

$$qbest_d = [qbest_{d1}, qbest_{d2}, \cdots, qbest_{dk}]^T \tag{20}$$

where d is the no. of the optimal particle $qbest$.

Step 5: the particles evolve according to Eqs. (21) and (22). Their positions are corrected:

$$v_t^{r+1} = w\cdot v_t^r + c_1\cdot r_1\cdot(pbest_d - X_t^r) + c_2\cdot r_2\cdot(qbest_d - X_t^r) \tag{21}$$

$$x_t^{r+1} = x_t^r + v_t^{r+1} \tag{22}$$

where w refers to the inertia weight of the flying speed of the particle; c_1 and c_2 are the learning factors; r_1 and r_2 are the random numbers in the interval [0, 1]; v_t^r is the flying speed of the particle in the process of the rth

iteration. The paper adopts the characteristics of random variable to adjust inertia weight; it is conducive to maintaining the diversity of population and jumping out of local optimum quickly as well as improving the global search performance of the algorithm. The calculation method of w is as follows:

$$\omega = \mu_{\min} + (\mu_{\max} - \mu_{\min}) \cdot rand() \tag{23}$$

where $\mu_{\min}$ and $\mu_{\max}$ are minimum and maximum of random inertia weight, $rand()$ is random number between 0 and 1.

Learning factor c_1 and c_2 control the particle ability of "self-awareness" and "social understanding", respectively. At the early period of the algorithm, c_1 and c_2 may enhance the global optimization ability by assigning larger and smaller values. On the contrary, c_1 and c_2 are advantageous to the algorithm converge to global optimal solution by assigning smaller and larger values at the late of algorithm searching. The calculation method of c_1 and c_2 are as follows:

$$\begin{cases} c_1 = c_{1,ini} - (c_{1,ini} - c_{1,fin})(t/T_{\max}) \\ c_2 = c_{2,ini} - (c_{2,fin} - c_{2,ini})(t/T_{\max}) \end{cases}$$

where $c_{1,ini}$ and $c_{2,ini}$ are the initial value of learning factor, $c_{1,fin}$ and $c_{2,fin}$ are the iterative final value of learning factor, t is the current number of iterations, $T_{\max}$ is the largest number of iterations.

In order to prevent the premature convergence problem occur during the process of iteration. The paper adopts population fitness variance σ^2 of particle swarm as the condition of premature judgment:

$$\sigma^2 = \sum_{x=1}^{m} (Fit(x) - Fit_{avg})^2 \leqslant H \tag{25}$$

where Fit_{avg} is the average fitness of current population; H is the maximum thresholds given by the system. If current status meet the condition of formula 25, the procedure come into premature convergence process, define "inert particles" from the current population according to formula (26) and take mutation operators to update the position of "inert particles" according to formula (27).

$$|Fit(x) - Fit(qbest_d)| \geqslant \sigma_1 \tag{26}$$

$$x_{i,j} = rand() \times \left(x_j^{\max} - x_j^{\min}\right) + x_j^{\min} \tag{27}$$

where $Fit(qbest_d)$ is the fitness of optimal particle; σ_1 is the minimum thresholds given by the system; $rand()$ is the random number between 0 and 1; $x_{i,j}$ is the new position of ith particle at jth dimension; $x_j^{\max}$ and $x_j^{\min}$ are the theory of maximum and minimum value at jth dimension.

Step 6: repeat step 3 to step 5 until it meets the number of iterations *iter* set by the system.

Step 7: stop the iteration, and find out the particle with the highest fitness at present. The position vector of the particle is the output coordination result of each Agent.

4.3. Process of energy coordination

When the original power supply and demand balance of the power generation unit is broken, any Agent whose state changes can apply to be a Task Agent to initiate the energy coordination task. The process of the coordination control algorithm is shown in Fig. 6, mainly including the following steps:

Step 1: release the bidding information.

Considering the CPU utilization and memory utilization index (Long et al., 2011), select Task Agent (load balance) from the Agents applying for the energy coordination task. After obtaining the time-stamped Task Token, Task Agent searches the current load and electricity price from LD Agent and sends the bid invitation to other Agents.

Step 2: agent enters a bid.

Each Agent organizes the tendering information based on the characteristics designed in Section 3.2 and submits the quad data $<E, B, C, S>$ before the prescribed deadline.

Step 3: Task Agent evaluates the bid.

After receiving the bidding information, Task Agent will make the global energy coordination control with the improved particle swarm algorithm stated in Section 4.2.

Step 4: find the bidding result.

Release the bidding result and the energy coordination control plan.

Step 5: Agent replies whether it has finished the task or not; if yes, the negotiation ends and Task Token fails; if not, re-initiate the energy coordination task.

5. Case study

5.1. Simulation environment

This paper designs MAS with Java Agent DEvelopment (JADE) which is a FIPA (The Foundation for Intelligent Physical Agents) standard-based multi-Agent software development framework with the following functions:

(1) Agent management system (AMS): responsible for controlling the activities and life cycle of Agent in the platform and the interaction between the external application and the platform, and identifying the name of Agent.

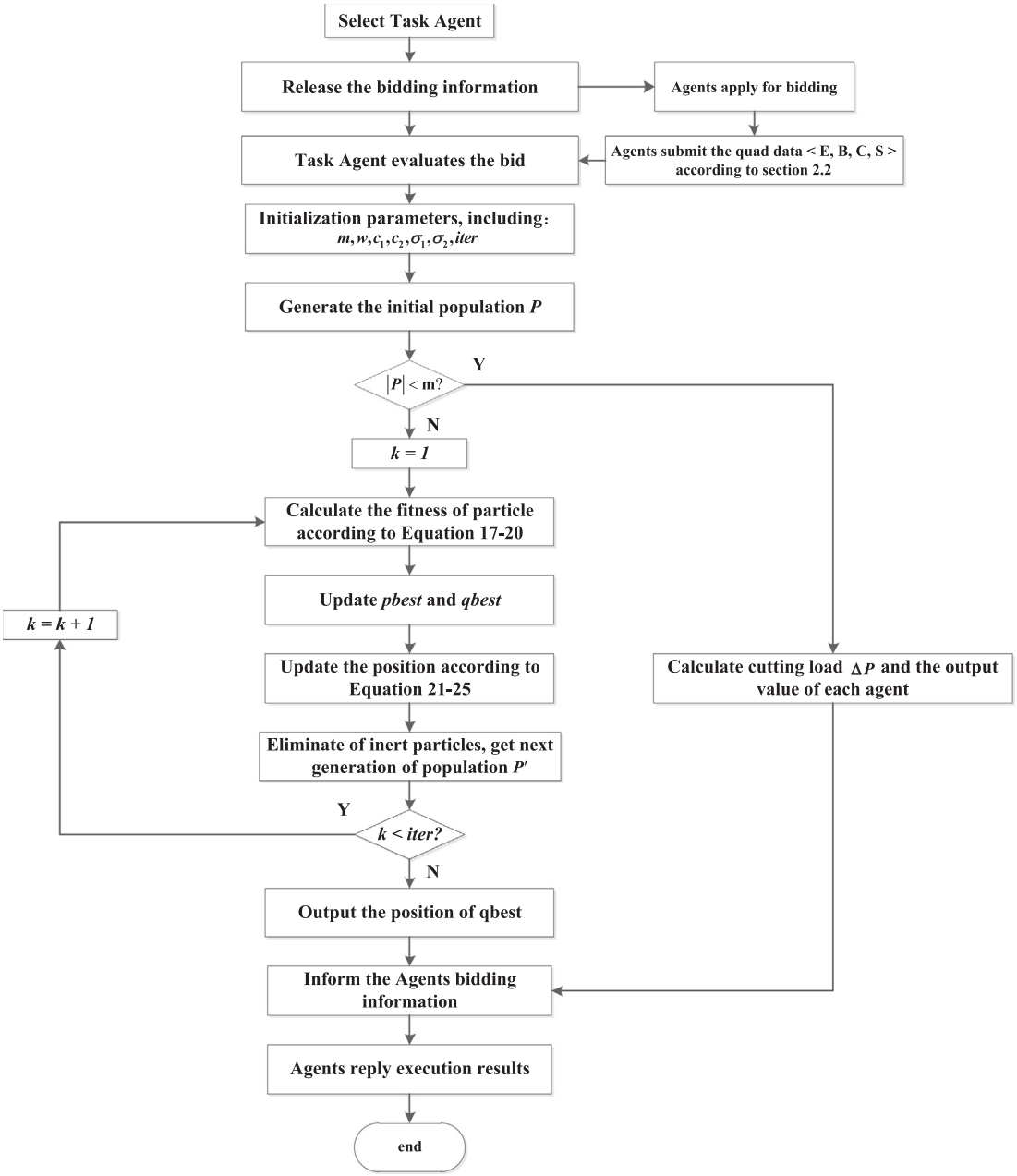

Fig. 6. The process of the coordination control algorithm.

(2) Directory Facilitator (DF): responsible for providing the yellow page service for Agents in the platform and registering the service type for searching.
(3) Agent Communication Channel (ACC): controlling the information transmission, encoding and analysis in the platform or among different platforms.

5.2. Basic data

The structure of the WPS-PGUs case study designed in the paper is shown in Fig. 7, in which WG1 to WG4 represent the single wind turbines; PU1 to PU4 represent one photovoltaic unit is formed by connecting several photovoltaic panels of the same type to the independent inverter chamber through the feeder. BAT1 to BAT4 represent one battery energy storage unit is formed by connecting several battery cabinets into a battery pack series and then connecting other battery pack series in parallel. BAT1 and BAT2 are the vanadium flow batteries which are controlled by ECO-BAT; BAT3 and BAT4 are the phosphoric acid iron batteries which are controlled by EME-BAT. The specifications of the equipment are shown in Table 2. The total installed capacities of wind/photovoltaic/energy storage are 9 MW/8.16 MW/5 MW, respectively.

The place for simulation is Zhangbei County in Zhangjiakou City, Hebei Province (114°21′E, 40°59′N). The load demand and meteorological conditions are taken as shown in Figs. 8–10. With 1 h as the calculation step, the time sharing electrovalence is shown in Table 3.

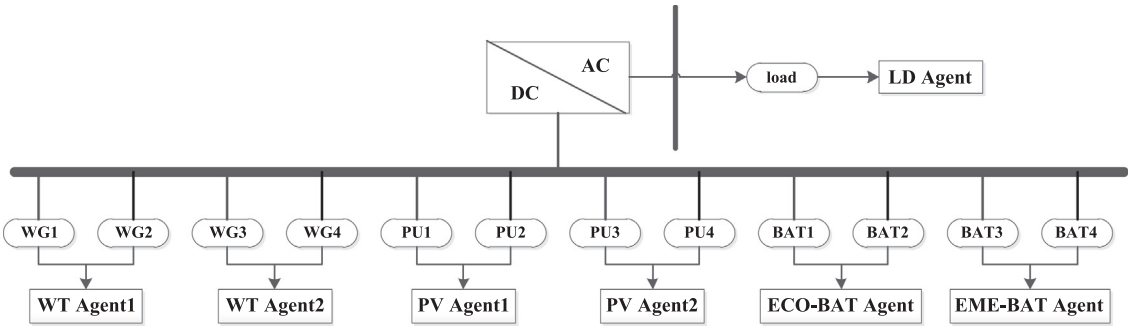

Fig. 7. The structure of the WPS-PGUs case study.

Table 2
The specifications of the equipment.

Wind turbine			PV panel		
Parameter	WG1/WG2	WG3/WG4	Parameter	PV1/PV2	PV3/PV4
Cut-in speed (m/s)	4	3	Peak power (MWp)	2.24	1.84
Rate wind speed (m/s)	12	11	MPPT voltage/current (V/A)	25.2/7.95	45/5.11
Rate power (MW)	2.5	2.0	Open-circuit voltage (V)	44.8	55.31
Hub height (m)	90	80	Short-circuit current (A)	8.33	5.48
ECO-BAT			EME-BAT		
Parameter	BAT1/BAT2		Parameter	BAT3/BAT4	
Maximum charge depth (%)	75		Maximum charge depth (%)	70	
Rated capacity (MW h)	2		Rated capacity (MW h)	3	
Maximum power (MW)	1		Maximum power (MW)	1.5	
Charge/discharge efficiency (%)	0.85/0.9		Charge/discharge efficiency (%)	0.9/0.95	

5.3. Results and analysis

5.3.1. Equipment output analysis

The multi-Agent system designed by Jun et al. (2011) (Scheme 1) and that designed in the paper (Scheme 2) are adopted for simulation to obtain the equipment output curve, as shown in Figs. 11 and 12:

RE in the figures represents the joint output curve of wind power and photovoltaic power. As Scheme 1 does not classify the batteries, Fig. 11 just presents the overall output curve of the batteries. It can be found by comparing RE output curves that the wind/photovoltaic utilization principles of two models are not completely consistent, that is because all the wind turbines and photovoltaic equipment in Scheme 1 work in MPPT (Maximum Power Point Tracking) (Chekired et al., 2014) mode and absorb all wind and photovoltaic resources to achieve the maximum renewable energy utilization; Scheme 2 is the result of optimizing the overall energy distribution under the premise of considering the life expectancy loss of the battery and time-of-use electricity price, which may reasonably abandon the utilization of part of renewable energies to make the overall economic benefit of the system better. It can be seen by comparing the battery output curve of two models that the charge and discharge of all batteries in Scheme 1 are controlled according to the difference between the load demand and the RE output, and the batteries are charged and discharged for many times; two types of batteries designed in Scheme 2 have different charge and discharge characteristics: the charge and discharge strategy of ECO-BAT is determined by the time-of-use electricity price and its own capacity, so the output is relatively stable without the frequent charge and discharge. EME-BAT is charged and discharged frequently, because it needs to determine its own charge and discharge control according to the outputs of load, RE and ECO-BAT. However, as part of the renewable energies are abandoned in the global optimization strategy, and the output of ECO-BAT reduces the difference between the outputs of load and RE, EME-BAT is not charged and discharged too often. The battery capacity curves are shown in Figs. 13 and 14:

It can be found by comparing the battery capacity curves of two models in Figs. 13 and 14 that: the capacity in Scheme 1 does not change greatly. This is because the energy consumption in the process of charging and discharging due to the large capacity base of the battery. Then, the frequent charge and discharge has little influence on the capacity; the capacity curves of two kinds of batteries are not the same in Scheme 2. The capacity of ECO-BAT tends to be stable in a certain range, which is because no frequent extreme requiring the batteries to be fully charged or worn out appears when controlling the charge and discharge according to the fuzzy control rules in Table 1 due to the short period of time in the peak and

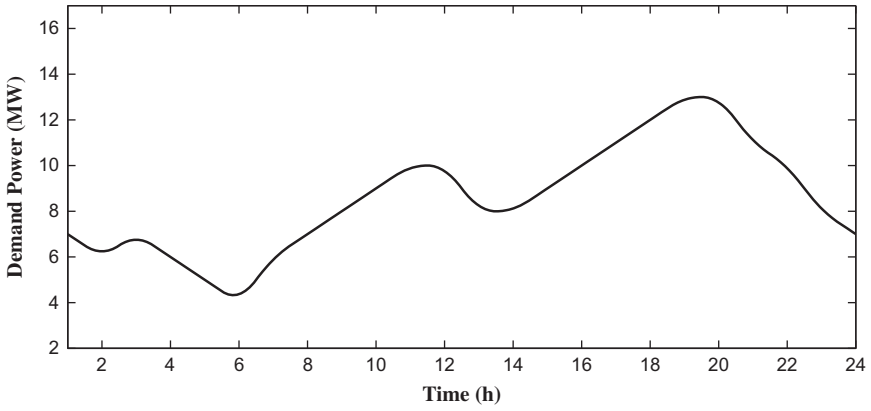

Fig. 8. The load demand curve.

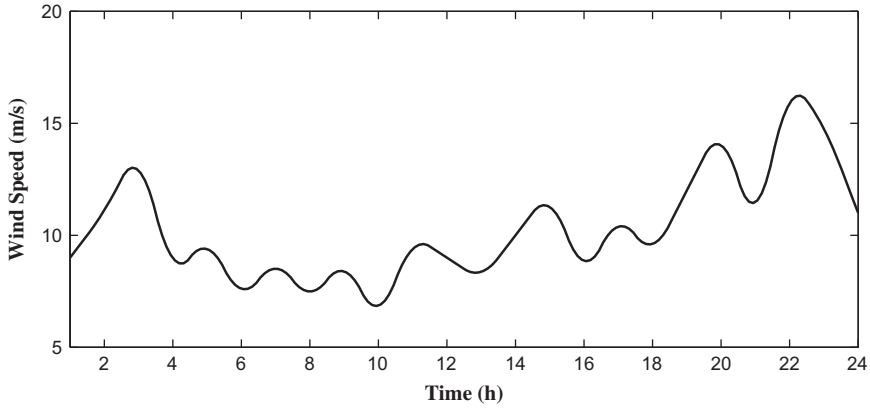

Fig. 9. The wind speed curve.

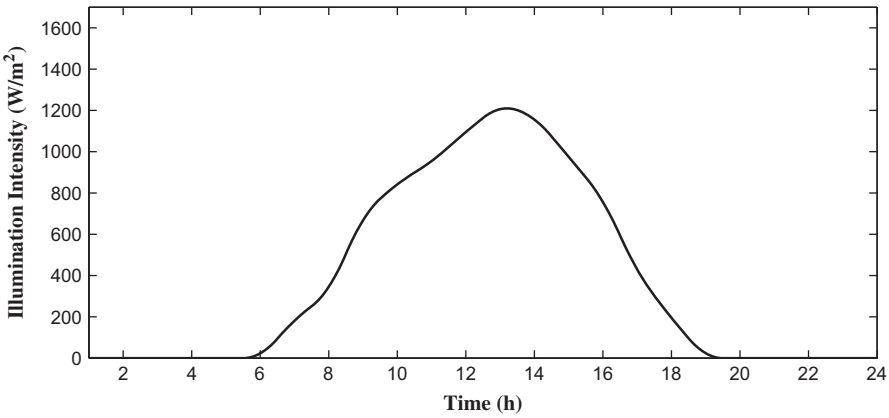

Fig. 10. The illumination intensity curve.

Table 3
The time sharing electrovalence.

Period	Time (h)	Price (US $/kW h)
Peak time	18–21	0.23
Usual time	0–6	0.18
Valley time	7–17, 22–23	0.13

valley load. The capacity of EME-BAT changes greatly. This is because each battery pack shares a large amount of task in the charging and discharging process due to the small capacity base. As a result, the frequent charge and discharge has great influence on the capacity.

5.3.2. Agent communication analysis

Take 3th time intervals as an example and combine the information communication map in Fig. 15 to illustrate the MAS energy coordination process. The whole energy coordination can be divided into the following six stages:

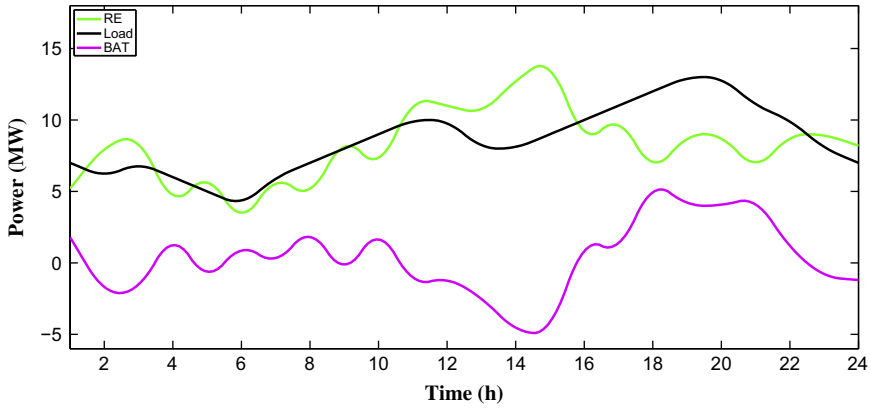

Fig. 11. The equipment output curve of Scheme 1.

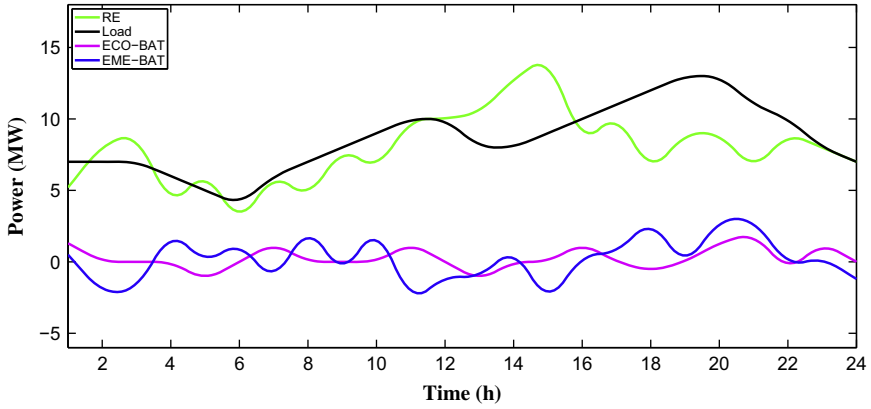

Fig. 12. The equipment output curve of Scheme 2.

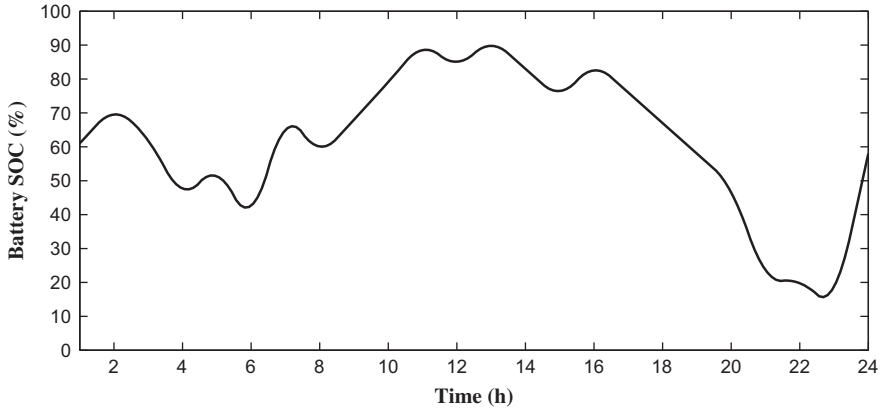

Fig. 13. Battery SOC of Scheme 1.

Stage 1: apply for Task Agent.

Both the wind speed and the load change in the third time interval. At this time, WT Agent1, WT Agent2 and LD Agent send the application for Task Agent to DF Agent and provide the CPU and memory utilization of the current Agent. DF Agent considers the load balance to distribute the Task Token with the Agent identity and timestamp and informs LD Agent.

Stage 2: initiate the bid invitation.

Task Agent searches the current load size and the power purchase price (LD Agent can search the information in

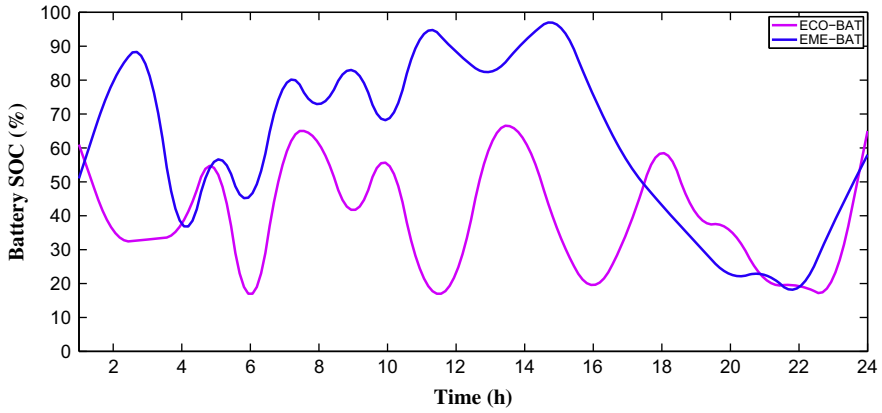

Fig. 14. Battery SOC of Scheme 2.

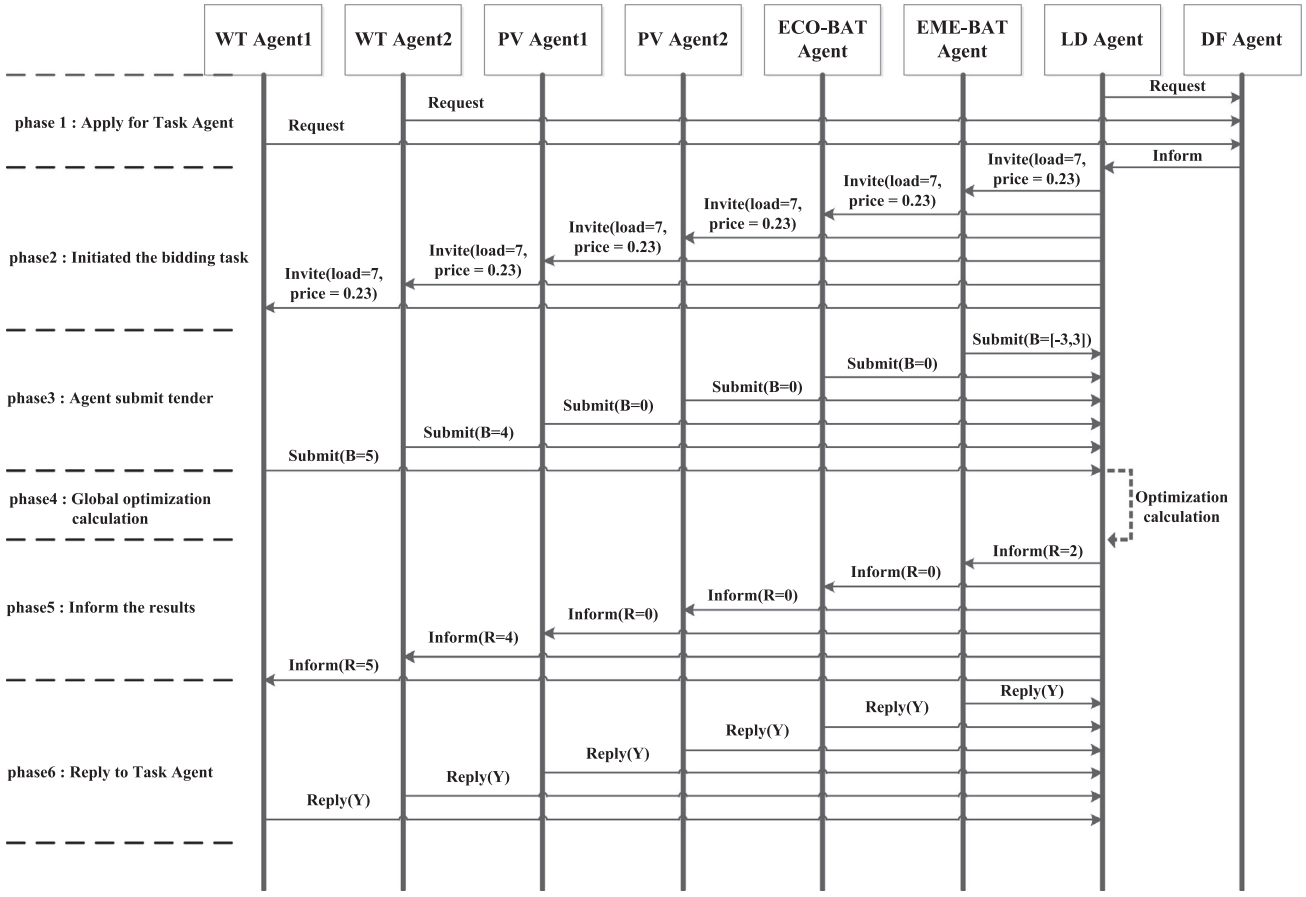

Fig. 15. MAS energy coordination process in 3th time intervals.

the local place.), releases the energy coordination bidding information, and sends the current load size (7 MW) and power price (0.13 $/kW h) to other Agents.

Stage 3: Agents enter the bid.

Each Agent makes the local decisions according to the characteristics of Agent introduced in Section 2.2, organizes the quad data $<E, B, C, S>$, in which the bid values B of WT Agent1, WT Agent2, PV Agent1, PV Agent2 and ECO-BAT Agent are 5 MW, 4 MW, 0 MW, 0 MW and 0 MW, respectively. The bid value of EME-BAT Agent is [−3, 3] MW. The information is sent to Task Agent after being packaged.

Stage 4: Task Agent makes the global energy coordination.

Task Agent stops receiving the bid information at the deadline, and calculates the outputs of each Agent based

Table 4
Economic indicators of two models.

Scheme	Income (US$)	Operating cost (US$)	Depreciation expense (US$)	Punishment cost (US$)	Earnings (US$)
Scheme 1	37,560	237.5	14,966	0	22,356.5
Scheme 2	37,560	166.7	11,372	0	26,021.3

on the global energy coordination control algorithm in Section 3.2. The bid values of WT Agent1, WT Agent2 and EME-BAT Agent are 5 MW, 4 MW and −2 MW, and that of other Agents is 0.

Stage 5: release the bidding result.

Immediately inform Agents of the energy distribution results. R refers to the final bidding result.

Stage 6: reply Task Agent.

Each Agent receives the bidding result and gives the corresponding control instruction to make the output of the equipment meet the requirements of Task Agent. If adjusting it successfully, it replies Yes (Y) to Task Agent; otherwise, it replies No (N). At this time, Task Agent re-initiates the energy coordination task. It can be seen from Fig. 15 that all Agents reply Yes.

5.3.3. Economic analysis

The amount of profits is one of the important factors for the popularization and application of the new energy power plants. Table 4 shows the economic indicators of two models:

According to the calculation results in Table 4, the MAS energy coordination control system proposed in the paper can reduce the operation cost and depreciation cost of the system. This part of costs is used to prolong the service life of the batteries on the basis of optimizing the charging and discharging strategies of the batteries to increase the overall economy of the system. By contrast, the profit of the method proposed in the paper increases by 16.4%.

6. Conclusions

A multi-agent-based energy-coordination control system for large-scale wind, photovoltaic, energy storage, and power-generation units is designed in this study. By building on the non-fixed client–server cooperative mechanism in the distributed environment, the system enhances flexibility and extensibility, avoids the single point of failure in the centralized control system, and increases operation stability. The proposed system uses the contract network protocol as the communication mechanism among agents and solves the global optimal-energy distribution plan by using the improved particle swarm algorithm by considering the self-constraints and interests of each part. On the basis of the characteristic analysis of different equipment, this study designs the WT, PV, ECO-BAT, EME-BAT, and LD agents, as well as the control objective and decision making methods of all kinds of agents, to enable agents to make decisions independently according to the environment. By using a power-generation unit in Zhangbei County in China as an example, this paper presents a simulation via the JADE platform to analyze the output characteristics of equipment under the energy-coordination control of the system, as well as the behavior characteristics and communication negotiation process of the agents. The results show that the system designed in the paper has good applicability in energy-coordination control and gains an advantage in the optimization of economic benefit. Therefore, the system designed in this paper is a good energy-coordination control plan in the large-scale utilization of renewable energy.

Acknowledgments

This work was sponsored by State Key Laboratory of Alternate Electrical Power System with Renewable Energy Sources (North China Electric Power University) and the Fundamental Research Funds for the Central Universities (No. 2014XS39).

References

Askarzadeh, A., 2013. Developing a discrete harmony search algorithm for size optimization of wind–photovoltaic hybrid energy system. Sol. Energy 98, 190–195.

Bayod-Rújula, Á.A., Haro-Larrodé, M.E., Martínez-Gracia, A., 2013. Sizing criteria of hybrid photovoltaic–wind systems with battery storage and self-consumption considering interaction with the grid. Sol. Energy 98, 582–591.

Campoccia, A., Dusonchet, L., Telaretti, E., Zizzo, G., 2009. Comparative analysis of different supporting measures for the production of electrical energy by solar PV and wind systems: four representative European cases. Sol. Energy 83 (3), 287–297.

Chekired, F., Mellit, A., Kalogirou, S.A., et al., 2014. Intelligent maximum power point trackers for photovoltaic applications using FPGA chip: a comparative study. Sol. Energy 101, 83–99.

da Rosa, M.A., Leite da Silva, A.M., Miranda, V., 2012. Multi-agent systems applied to reliability assessment of power systems. Int. J. Electr. Power Energy Syst. 42 (1), 367–374.

Dimeas, A.L., Hatziargyriou, N.D., 2005. Operation of a multiagent system for microgrid control. IEEE Trans. Power Syst. 20 (3), 1447–1455.

Ding, M., Luo, K., Bi, R., 2013. An energy coordination control strategy for islanded microgrid based on a multi-agent system. Dianli Xitong Zidonghua (Automat. Electr. Power Syst.) 37 (5).

Dufo-Lopez, R., Bernal-Agustin, J.L., 2008. Multi-objective design of PV–wind–diesel–hydrogen–battery systems. Renew. Energy 33 (12), 2559–2572.

Eberhart, R., Kennedy, J., 1995. A new optimizer using particle swarm theory. In: Micro Machine and Human Science. MHS'95, Proceedings of the Sixth International Symposium on IEEE, 1995, pp. 39–43.

Golovanov, N., Lazaroiu, G.C., Roscia, M., Zaninelli, D., 2013. Power quality assessment in small scale renewable energy sources supplying distribution systems. Energies 6 (2), 634–645.

Java Agent Development Framework. <http://jade.tilab.com/>.
Jiang, Z., 2008. Agent-based power sharing scheme for active hybrid power sources. J. Power Sources 177 (1), 231–238.
Jun, Z., Junfeng, L., Jie, W., Ngan, H.W., 2011. A multi-agent solution to energy management in hybrid renewable energy generation system. Renew. Energy 36 (5), 1352–1363.
Kazem, H.A., Khatib, T., 2013. A novel numerical algorithm for optimal sizing of a photovoltaic/wind/diesel generator/battery microgrid using loss of load probability index. Int. J. Photoenergy.
Kremers, E., Gonzalez de Durana, J., Barambones, O., 2013. Multi-agent modeling for the simulation of a simple smart microgrid. Energy Convers. Manage. 75, 643–650.
Lagorse, J., Simões, M.G., Miraoui, A., 2009. A multiagent fuzzy-logic-based energy management of hybrid systems. IEEE Trans. Ind. Appl. 45 (6), 2123–2129.
Lagorse, J., Paire, D., Miraoui, A., 2010. A multi-agent system for energy management of distributed power sources. Renew. Energy 35 (1), 174–182.
Li, J., Wei, W., Xiang, J., 2012. A simple sizing algorithm for stand-alone PV/wind/battery hybrid microgrids. Energies 5 (12), 5307–5323.
Logenthiran, T., Srinivasan, D., Wong, D., 2008. Multi-agent coordination for DER in MicroGrid. In: IEEE International Conference on Sustainable Energy Technologies, 2008. ICSET, 2008, pp. 77–82.
Logenthiran, T., Srinivasan, D., Khambadkone, A.M., 2011. Multi-agent system for energy resource scheduling of integrated microgrids in a distributed system. Electr. Power Syst. Res. 81 (1), 138–148.
Long, Q., Lin, J., Sun, Z., 2011. Agent scheduling model for adaptive dynamic load balancing in agent-based distributed simulations. Simul. Model. Pract. Theory 19 (4), 1021–1034.
Merei, G., Berger, C., Sauer, D.U., 2013. Optimization of an off-grid hybrid PV–wind–diesel system with different battery technologies using genetic algorithm. Sol. Energy 97, 460–473.
Mohammadi, M., Hosseinian, S.H., Gharehpetian, G.B., 2012. Optimization of hybrid solar energy sources/wind turbine systems integrated to utility grids as microgrid (MG) under pool/bilateral/hybrid electricity market using PSO. Sol. Energy 86 (1), 112–125.
Pipattanasomporn, M., Feroze, H., Rahman, S., 2012. Securing critical loads in a PV-based microgrid with a multi-agent system. Renew. Energy 39 (1), 166–174.
Roche, R., Idoumghar, L., Suryanarayanan, S., Daggag, M., Solacolu, C.A., Miraoui, A., 2012. A flexible and efficient multi-agent gas turbine power plant energy management system with economic and environmental constraints. Appl. Energy.
Smith, R.G., 1980. The contract net protocol: high-level communication and control in a distributed problem solver. IEEE Trans. Comput. 100 (12), 1104–1113.
Yang, H., Lu, L., Zhou, W., 2007. A novel optimization sizing model for hybrid solar–wind power generation system. Sol. Energy 81 (1), 76–84.
Yang, H., Wei, Z., Chengzhi, L., 2009. Optimal design and techno-economic analysis of a hybrid solar–wind power generation system. Appl. Energy 86 (2), 163–169.